

Compact Stars with Sequential QCD Phase Transitions

Mark Alford¹ and Armen Sedrakian²

¹ *Department of Physics, Washington University, St Louis, MO 63130, USA*

² *Frankfurt Institute for Advanced Studies, D-60438 Frankfurt-Main, Germany*

Compact stars may contain quark matter in their interiors at densities exceeding several times the nuclear saturation density. We explore models of such compact stars where there are two first-order phase transitions: the first from nuclear matter to a quark-matter phase, followed at higher density by another first-order transition to a different quark matter phase [e.g., from the two-flavor color superconducting (2SC) to the color-flavor-locked (CFL) phase]. We show that this can give rise to two separate branches of hybrid stars, separated from each other and from the nuclear branch by instability regions and, therefore, to a new family of compact stars, denser than the ordinary hybrid stars. In a range of parameters, one may obtain twin hybrid stars (hybrid stars with the same masses but different radii) and even triplets where three stars, with inner cores of nuclear matter, 2SC matter, and CFL matter, respectively, all have the same mass but different radii.

1. Introduction.— Compact stars are formed in the last stages of stellar evolution, their distinctive feature being that they are in gravitational equilibrium supported by the quantum pressure of degenerate fermionic matter. The less dense of such objects, white dwarfs, are supported by electron degeneracy pressure; the second densest class, neutron stars, are supported by the degeneracy pressure of interacting nucleonic (baryonic) matter. It has been conjectured long ago [1–4] that a higher-density class of compact stars may arise in the form of hybrid (or quark) stars, whose core (or entire volume) consists of quark matter. It has been previously noted [5–10] that the hybrid stars may form a separate branch (third family) of compact stars, separated from neutron stars by an instability region analogous to the one existing between white dwarfs and neutron stars. Such an elucidation of the relationship between the phases of high-density matter and the observable properties of compact stars helps to address one of the key challenges of strong interaction physics, which is to constrain, from theory and experiment, the phase diagram of ultradense matter.

NASA’s NICER experiment, to become operative in 2017 [11], will allow measurements of neutron star masses and, especially, radii to unprecedented precision with better than 10% uncertainty. Its capability of rotation-resolved spectroscopy of the thermal and nonthermal emissions of neutron stars in the soft (0.2–12 keV) x-ray band is expected to provide new insights into key properties of neutron stars, in particular constraints on the mass-radius relation. The measurements of the radii of neutron stars in combination with the previously established lower limit on the maximum mass of compact stars which is in the range $1.93(2) M_{\odot}$ [12, 13] to $2.01(4) M_{\odot}$ [14] will strengthen existing constraints on the equation of state (EOS) of ultradense matter.

The main body of research on hybrid compact stars, i.e., stars that are composed of a quark core surrounded by a nuclear envelope (which in turn is composed minimally of a liquid core and a crust) has concentrated on the case where the quark-matter core is represented by

a single phase (for recent reviews see [15, 16]). However, as our understanding of the QCD phase diagram improved over the years it became clear that the quark core may contain layers of distinct phases such as the various color superconducting phases of deconfined quark matter [17, 18]. It is generally agreed that the color-flavor-locked (CFL) phase will occur in the QCD phase diagram at sufficiently high densities, but different quark-matter phases may occur at intermediate densities, such as the two-flavor color-superconducting (2SC) phase and related phases [19–22], unpaired quark matter [23], or other alternatives [24]. The stability of the star sequences which develop CFL matter cores has been questioned in studies based on the Nambu–Jona-Lasinio model [25–27], but additional repulsive vector interaction appears to stabilize stars with CFL cores [22]. Generically, repulsive interaction in high-density (unpaired) quark matter leads also to high-mass twin stars with and without strangeness degrees of freedom [28–33], observations of which may serve as evidence of the existence of a critical end point in the QCD phase diagram [34, 35].

At densities near or below nuclear saturation density ($n_{\text{sat}} = 0.16 \text{ fm}^{-3}$), we use a “natural” EOS, constructed from a Lagrangian (or Hamiltonian) that is fitted to nuclear phenomenology. At higher densities, we allow for two sharp first-order phase transitions, assuming that mixed phases are disfavored by surface tension and electrostatic energy costs [30, 36–38]. Since the phase structure in that region is unknown, we use a “synthetic” EOS via a “CSS” parameterization [39] in which each quark-matter phase is assumed to have a constant (density-independent) speed of sound [39–41]. This can describe the two sequential phase transitions in terms of six parameters (see below). In this parameter space we explore the implications of such phase transitions for the masses and radii of compact stars. We find that the second phase transition can lead to a new branch (fourth family) of compact stars, which in turn gives rise to new phenomena such as twin configurations where both members are hybrid stars and even triplets consisting of three

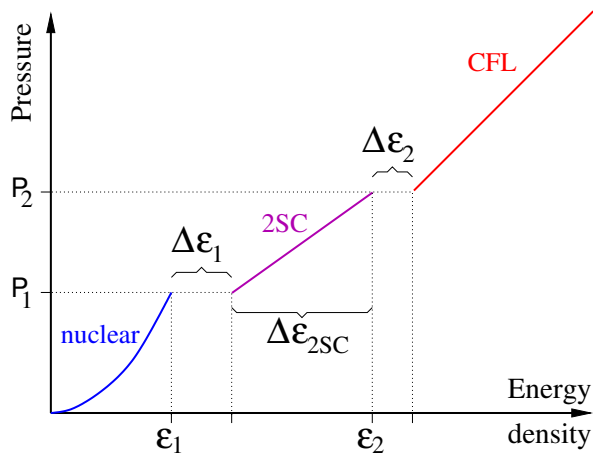


FIG. 1: Schematic plot showing how we parametrize the EOS of dense matter with two phase transitions to two quark-matter phases. For convenience and specificity, we call the first quark-matter phase 2SC and the second CFL.

distinct configurations with the same mass, but different radii and internal composition.

2. *Generating synthetic equations of state.*— The parameters of our EOS are illustrated in Fig. 1. For nuclear matter we use the “DDME2” EOS which is based on density-dependent relativistic functional theory [42]. This EOS fulfills the constraints derived from the heavy ion collisions and other terrestrial experiments, see Fig. 12 of Ref. [43]. It produces nucleonic compact stars with a maximum gravitational mass $M \simeq 2.3 M_\odot$, where M_\odot is the solar mass. The quark-matter EOS is parametrized by [39]

- (i) P_1 and P_2 (or, equivalently, P_1 and $\Delta\varepsilon_{2SC}$), the transition pressures for the nuclear \rightarrow 2SC and 2SC \rightarrow CFL transitions;
- (ii) $\Delta\varepsilon_1$ and $\Delta\varepsilon_2$, the magnitudes of the jumps in the energy density at these two phase transitions; and
- (iii) the squared sound speeds s_1 and s_2 in the 2SC and CFL phases. Causality requires $s_{1,2} \leq 1$.

The analytic form of the quark-matter EOS is

$$P(\varepsilon) = \begin{cases} P_1, & \varepsilon_1 < \varepsilon < \varepsilon_1 + \Delta\varepsilon_1 \\ P_1 + s_1[\varepsilon - (\varepsilon_1 + \Delta\varepsilon_1)], & \varepsilon_1 + \Delta\varepsilon_1 < \varepsilon < \varepsilon_2 \\ P_2, & \varepsilon_2 < \varepsilon < \varepsilon_2 + \Delta\varepsilon_2 \\ P_2 + s_2[\varepsilon - (\varepsilon_2 + \Delta\varepsilon_2)], & \varepsilon > \varepsilon_2 + \Delta\varepsilon_2. \end{cases} \quad (1)$$

3. *Mass-radius relations of compact stars.* — We solved the general relativistic structure equations of compact stars [44, 45] for our model EOS (1) for spherically symmetric (nonrotating and nonmagnetized) stars. We look for stable configurations using the Bardeen-Thorne-Meltzer criterion [46], which in our context states that a star is stable if the mass is rising with the central pressure. There may be other nonradial instabilities but we leave a study of these to future work.

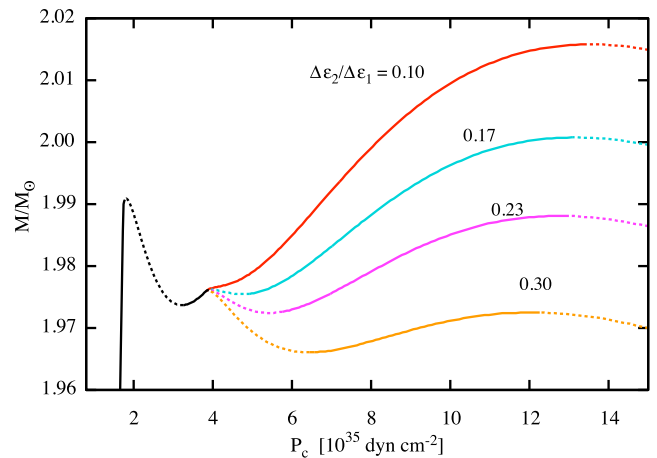


FIG. 2: The stellar mass as a function of the star’s central pressure for four different values of $\Delta\varepsilon_2$. The other parameters of the EOS are fixed at $P_1 = 1.7 \times 10^{35} \text{ dyn cm}^{-2}$, $s_1 = 0.7$, $\Delta\varepsilon_{2SC}/\varepsilon_1 = 0.27$, $\Delta\varepsilon_1/\varepsilon_1 = 0.6$, and $s_2 = 1$. The vertical dotted lines mark the two phase transitions at P_1 and P_2 . Stable branches are solid lines, unstable branches are dashed lines. We see the emergence of separate 2SC and CFL hybrid branches along with the occurrence of triplets.

We first explore a scenario where both the quark-matter equations of state are fairly stiff, with $s_1 = 0.7$ and $s_2 = 1$; we will discuss a softer EOS for the 2SC phase below. We fix the nuclear \rightarrow 2SC transition at $P_1 = 1.7 \times 10^{35} \text{ dyn cm}^{-2}$, corresponding to nucleonic energy density $\varepsilon_1 = 8.34 \times 10^{14} \text{ g cm}^{-3}$ and baryon density $n_1 = 3.0n_{\text{sat}}$. This means that the mass of the star reaches $M = 1.99 M_\odot$ before any transition to quark matter occurs, ensuring that all our mass-radius curves obey the observational lower bound on the maximum mass of a neutron star which is in the range $1.93(2) M_\odot$ [12, 13] to $2.01(4) M_\odot$ [14]. There remain three parameters to fix: the width of the 2SC phase $\Delta\varepsilon_{2SC}$ and the two energy-density jumps $\Delta\varepsilon_1$ and $\Delta\varepsilon_2$.

Figure 2 shows the mass as a function of the central pressure for four sequences of stars parametrized as follows. We have fixed the width of the 2SC phase $\Delta\varepsilon_{2SC}/\varepsilon_1 = 0.27$ and the energy-density jump at the nuclear \rightarrow 2SC transition $\Delta\varepsilon_1/\varepsilon_1 = 0.6$, and the four sequences have different values of the energy-density jump $\Delta\varepsilon_2$ at the 2SC \rightarrow CFL transition.

Our choice of values of P_1 , $\Delta\varepsilon_1$, and s_1 leads to the occurrence of a disconnected branch of stars with 2SC cores. In the figure, we see that, when the central pressure rises above P_1 , and 2SC quark matter appears in the core, the star becomes unstable (dashed black line), but then at $P_c = 3.2 \times 10^{35} \text{ dyn cm}^{-2}$ the stable branch of 2SC hybrid stars begins (solid black line).

This sequence is then interrupted by the 2SC \rightarrow CFL phase transition at $P_2 = 3.11 \times 10^{35} \text{ dyn cm}^{-2}$, at which a CFL core appears at the center of the star, within

the existing 2SC core. If there is a small energy-density jump $\Delta\varepsilon_2$ at this transition the hybrid branch will continue (upper solid line). However, if $\Delta\varepsilon_2$ is large enough, then the appearance of the CFL core destabilizes the star again, until at a higher central pressure, thanks to the stiffness of the CFL phase ($s_2 = 1$), a new stable sequence emerges.

We see that for $\Delta\varepsilon_2/\Delta\varepsilon_1$ greater than about 0.15 there are two separate, disconnected hybrid branches, both of which are disconnected from the nucleonic branch of stars with $P_c < P_1$. The disconnected stable branch of stars with a CFL core constitutes a *fourth family* of compact stars, adding to white dwarfs (not shown), ordinary neutron stars (near-vertical black line at $P_c < P_1$) and 2SC hybrid stars (solid black line at P_c just below P_2).

Moreover, for certain values of $\Delta\varepsilon_2$ there exist *triplet configurations*: a set of three stars which have the same mass but different central pressures, compositions, and radii. In Fig. 2 this is particularly clear for $\Delta\varepsilon_2/\Delta\varepsilon_1 = 0.23$.

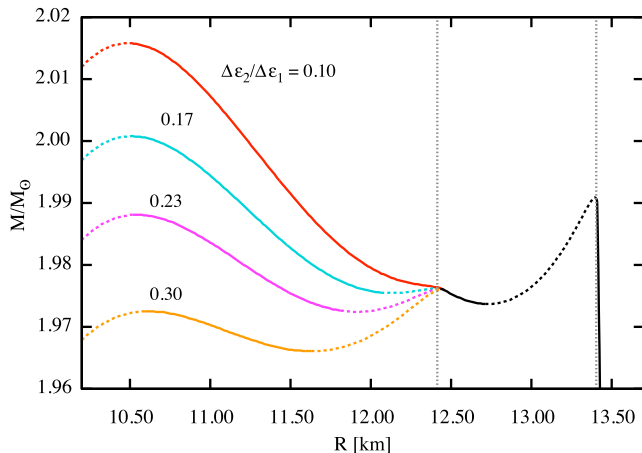


FIG. 3: The M - R relations for the parameter values defined in Fig. 2. We have fixed the properties of the nuclear \rightarrow 2SC transition and the speed of sound in 2SC and CFL matter. For the 2SC \rightarrow CFL transition we have fixed the critical pressure and we vary the energy-density discontinuity $\Delta\varepsilon_2$. The separate 2SC and CFL hybrid branches are clearly visible, along with the occurrence of triplets.

In Fig. 3 we show the mass-radius relation for the sequences shown in Fig. 2. The disconnected branches are, in principle, observable because they are separated by intervals of radius in which no star can exist. These disallowed intervals cover ranges of hundreds of meters, which is only slightly beyond the resolution of the measurements expected imminently from NICER, and would provide motivation for future efforts to make radius measurements more precise and increase the statistics. The observation of two stars with very different radii will be a hint of the presence of twins or triplets. In Fig. 3, the maximum separation between the nucleonic branch

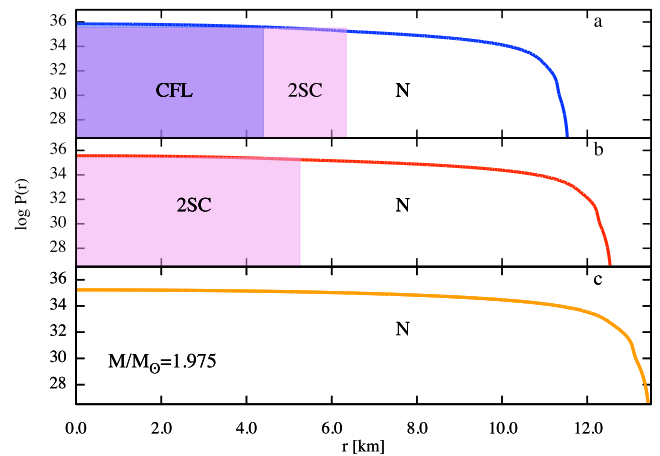


FIG. 4: The profiles (here the log of pressure as a function of the internal radius) of the three members of a triplet with masses $M = 1.975 M_\odot$. Here “N” means the nucleonic phase. The parameter values are the same as in Fig. 2, with $\Delta\varepsilon_2/\Delta\varepsilon_1 = 0.23$.

and the CFL branch is about 2 km, well within NICER’s resolution.

In Fig. 4, we show the profiles of the three members of the triplet of stars, all with mass $1.975 M_\odot$, that occur for the EOS parameter values used in Fig. 2, with $\Delta\varepsilon_2/\Delta\varepsilon_1 = 0.23$. The most compact member has a CFL core, and 2SC shell, with $R = 11.5$ km. The next has a 2SC core and $R = 12.5$ km. The purely nucleonic member has $R = 13.5$ km. The radii differ by 1–2 km, which is potentially detectable by NICER.

The results shown in Figs. 2 and 3 were for various values of $\Delta\varepsilon_2$ at fixed $\Delta\varepsilon_1/\varepsilon_1 = 0.6$. We now explore the effects of varying both $\Delta\varepsilon_1$ and $\Delta\varepsilon_2$. Our results are summarized in Table I. The notation describes the sequence of branches encountered as the central pressure rises from P_1 up through P_2 ; stable branches are denoted by “s” and unstable branches by “u.” A comma separates the 2SC sequence from the CFL sequence. For example, the top curve in Fig. 2 would be denoted us, s (unstable 2SC branch, stable 2SC branch, then a stable CFL branch). The bottom curve in Fig. 2 would be denoted us, us (unstable 2SC branch, stable 2SC branch, and then an unstable CFL branch, and then a stable CFL branch). Of course, all sequences eventually become unstable at a high enough central pressure: We take this as given and do not append a u to every denotation.

When both the phase transition are weakly first order, with small energy-density jumps (top left corner of Table I), the phase transitions do not induce instabilities [39, 40], so as the central pressure rises above P_1 there is a single continuous family of hybrid stars, denoted s, s , first with a 2SC core, and then with a CFL core inside that at the center enveloped by a 2SC shell.

When both the phase transitions are strongly first or-

$\Delta\varepsilon_2/\Delta\varepsilon_1$	$\Delta\varepsilon_1/\varepsilon_1$			
	0.4	0.5	0.6	0.7
0.1	s, s	s, s	$\underbrace{us, s}_{\text{N-2SC}}$	$\underbrace{u, us}_{\text{N-CFL}}$
0.2	s, s	s, s	$\underbrace{us, us}_{\text{triplet}}$	$\underbrace{u, us}_{\text{N-CFL}}$
0.3	s, s	s, s	$\underbrace{us, us}_{\text{N-2SC;N-CFL}}$	$\underbrace{u, us}_{\text{N-CFL}}$
0.4	s, s	$\underbrace{s, us}_{\text{2SC-CFL}}$	$\underbrace{us, u}_{\text{N-2SC}}$	u, u
0.5	s, s	$\underbrace{s, us}_{\text{2SC-CFL}}$	$\underbrace{us, u}_{\text{N-2SC}}$	u, u

TABLE I: Summary of the stability properties of compact star sequences as we vary the energy density discontinuities $\Delta\varepsilon_1$ and $\Delta\varepsilon_2$. See the text for an explanation of the notation. The presence of twin hybrid configurations or triplet configurations is marked by the square underbraces with information about the involved phases (“N” means nuclear). The fixed parameters P_1 , P_2 , s_1 , and s_2 are as in Figs. 2 and 3.

der (bottom right corner of Table I), the appearance of the denser phase tends to destabilize the star, and both the 2SC and CFL sequences are unstable (denoted as u, u).

From Table I, we see that the interesting phenomena illustrated in Figs. 2 and 3 arise as we vary the parameters of the EOS from the “ s, s ” domain (no unstable branches) to the “ u, u ” domain (no stable branches). In the intermediate parameter range, stability may be lost and regained twice, once within the 2SC sequence and once within the CFL sequence, creating the possibility of twin stars (with the same mass but different radius) or even triplets (three stars with the same mass but different radii). Three types of twins are possible: N-2SC (hybrid star with a 2SC core has the same mass as a nucleonic star), N-CFL (hybrid star with a 2SC outer core and a CFL inner core has the same mass as a nucleonic star), and 2SC-CFL (hybrid star with a 2SC core has the same mass as a hybrid star with a 2SC outer core and a CFL inner core).

The results above were obtained for stiff quark matter, with $s_1 = 0.7$ and $s_2 = 1$. We now explore how our results change if the 2SC phase is assumed to have a less stiff EOS with $s_1 = 0.5$, which is still somewhat above the expected value $s = 1/3$ for noninteracting massless quarks. The CFL phase remains maximally stiff, with $s_2 = 1$. We lower the nuclear \rightarrow 2SC transition pressure to $P_1 = 1.14 \times 10^{35}$ dyn cm $^{-2}$, corresponding to nucleonic energy density $\varepsilon_1 = 7.28 \times 10^{14}$ g cm $^{-3}$ and baryon density $n_1 = 2.6n_{\text{sat}}$. We set $\Delta\varepsilon_{2\text{SC}}/\varepsilon_1 = 0.15$, corresponding to $P_2 = 1.83 \times 10^{35}$ dyn cm $^{-2}$, and fix $\Delta\varepsilon_1/\varepsilon_1 = 0.6$.

In Fig. 5 we show a set of mass-radius curves for these parameter values, varying the energy-density discontinuity $\Delta\varepsilon_2$ at the 2SC \rightarrow CFL transition. In this case the nu-

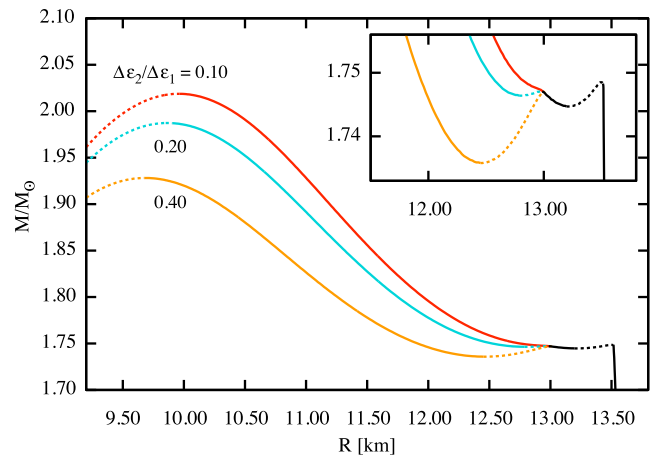


FIG. 5: The M - R relation for a less stiff 2SC phase ($s_1 = 0.5$) with four different values of $\Delta\varepsilon_2$, keeping $\Delta\varepsilon_1/\varepsilon_1 = 0.6$. The 2SC branch is shorter, but there can still be separate 2SC and CFL hybrid branches and triplets (the corresponding region is magnified in the figure inset).

cleonic branch ends at a mass of about $1.74 M_\odot$, but there are still families of stars that meet the maximum mass constraint. We see that the 2SC branch is shorter and shallower, but there can still be separate 2SC and CFL hybrid branches, and triplets, with “forbidden” ranges of radii covering several hundred meters.

A number of interesting astrophysical scenarios involve twins and by extension also triplets discussed above. One scenario involves a spin-up (in a binary) or spin-down (in isolation) induced QCD phase transition in a compact star which would be accompanied by a quick change in the star’s global properties. This could induce drastic (depending on how large the energy-density jump is) changes in spin, for example, backbending [47–49], or a release of large portions of gravitational binding energy in an explosion or collapse [50–52]. Core-collapse supernovas provide yet another setting where the QCD phase transition(s) can induce additional shock wave(s) [53] and affect the supernova outcome. These require an extension of the input EOS to finite temperatures; see, e.g., Ref. [54]. Finally, future detections of gravitational waves from binary neutron star inspirals and mergers may provide independent constraints on the radii and masses of compact objects; any density discontinuities in the EOS are likely to leave their distinctive imprint in the data which would reveal a phase transition(s) to QCD matter [55–60].

4. Conclusions and Outlook.— In this work, we investigated the physical consequences of assuming that there are two sequential first-order phase transitions in dense matter, first from a nucleonic phase to a quark-matter phase that for convenience we called 2SC and second from that phase to a denser quark-matter phase that we called CFL. (Such sequential first-order phase tran-

sitions emerge, for example, in QCD-inspired models of dense quark-matter [19–22]). By using simple constant-sound-speed parameterizations of the quark-matter EOS we were able to explore, at least partly, the spaces of possible EOS and the mass-radius properties of the resulting stellar sequences. The models were constrained to be causal ($s_{1,2} \leq 1$) and to satisfy the two-solar-mass observational constraint.

We found that if the quark matter is fairly stiff (the squared speed of sound being at least 0.5 in the 2SC phase, and 1 in CFL), then the sequence of two phase transitions can yield characteristic phenomena:

(a) Pairs of disconnected branches of hybrid stars, separated from each other and from the nucleonic stars by unstable intervals, corresponding to ranges of radii in which no stars can occur. This represents a new branch of compact stars (fourth family) which, for a given EOS, are denser than the hybrid stars that arise when there is a single phase transition from nucleonic to quark matter. (b) Connected with this, we find equal mass “twin” stars of the type N-2SC, N-CFL which could have been anticipated from the studies of ordinary hybrid stars, but also 2SC–CFL twins which both contain quark matter. (c) Triplet configurations: three equal-mass stars with different radii and internal structures.

In the future, it would be useful to perform a more comprehensive survey of the six-dimensional parameter space of our model, looking for regularities and systematic features, and to match the parameterization used in this study with models based on different classes of QCD models (ranging from the perturbative to QCD-inspired effective ones; see Refs. [15, 16], and references therein). Extrapolating from the current model, each additional first-order phase transitions may lead to another disconnected branch of compact stars. Imminent observational advances, in particular, the science program of the NICER experiment, are expected to provide further insight on the potentially complex structure of the compact stars that can exist in nature.

We thank D. Blaschke, Th. Klähn, M. Oertel, S. Reddy, S. Schramm, L. Tolós, F. Weber, and D. Zappalà for useful comments on the manuscript. M. A. is partly supported by the U.S. Department of Energy, Office of Science, Office of Nuclear Physics under Award No. #DE-FG02-05ER41375. A.S. is supported by the Deutsche Forschungsgemeinschaft (Grant No. SE 1836/3-2) and by NewCompStar COST Action MP1304.

[1] D. D. Ivanenko and D. F. Kurdgelaidze, *Astrophysics* **1**, 479 (1965).
 [2] F. Pacini, *Nature (London)* **209**, 389 (1966).
 [3] D. Boccaletti, V. de Sabbata, and C. Gualdi, *Nuovo Cimento* **45**, 513 (1966).
 [4] N. Itoh, *Prog. Theor. Phys.* **44**, 291 (1970).

[5] U. H. Gerlach, *Phys. Rev.* **172**, 1325 (1968).
 [6] R. L. Bowers, A. M. Gleeson, and R. D. Pedigo, *ApJ* **213**, 840 (1977).
 [7] B. Kämpfer, *J. of Phys. A* **14**, L471 (1981).
 [8] N. K. Glendenning and C. Kettner, *A&A* **353**, L9 (2000), [astro-ph/9807155](#).
 [9] K. Schertler, C. Greiner, J. Schaffner-Bielich, and M. H. Thoma, *Nucl. Phys.* **A677**, 463 (2000), [arXiv:astro-ph/0001467 \[astro-ph\]](#).
 [10] F. Weber, *Prog. in Part. Nucl. Phys.* **54**, 193 (2005), [astro-ph/0407155](#).
 [11] K. Gendreau, Z. Arzoumanian, and NICER Team, AAS Meeting (2017) No. 229, id. 309.03.
 [12] P. B. Demorest, T. Pennucci, S. M. Ransom, M. S. E. Roberts, and J. W. T. Hessels, *Nature* **467**, 1081 (2010), [arXiv:1010.5788 \[astro-ph.HE\]](#).
 [13] E. Fonseca *et al.*, *Astrophys. J.* **832**, 167 (2016), [arXiv:1603.00545 \[astro-ph.HE\]](#).
 [14] J. Antoniadis, P. C. C. Freire, N. Wex, T. M. Tauris, R. S. Lynch, M. H. van Kerkwijk, M. Kramer, C. Bassa, V. S. Dhillon, T. Driebe, J. W. T. Hessels, V. M. Kaspi, V. I. Kondratiev, N. Langer, T. R. Marsh, M. A. McLaughlin, T. T. Pennucci, S. M. Ransom, I. H. Stairs, J. van Leeuwen, J. P. W. Verbiest, and D. G. Whelan, *Science* **340**, 448 (2013), [arXiv:1304.6875 \[astro-ph.HE\]](#).
 [15] N. Brambilla, S. Eidelman, P. Foka, S. Gardner, A. S. Kronfeld, M. G. Alford, R. Alkofer, M. Butenschoen, T. D. Cohen, J. Erdmenger, L. Fabbietti, M. Faber, J. L. Goity, B. Ketzer, H. W. Lin, F. J. Llanes-Estrada, H. Meyer, P. Pakhlov, E. Pallante, M. I. Polikarpov, H. Satzjian, A. Schmitt, W. M. Snow, A. Vairo, R. Vogt, A. Vuorinen, H. Wittig, P. Arnold, P. Christakoglou, P. Di Nezza, Z. Fodor, X. G. i. Tormo, R. Höllwieser, A. Kalweit, D. Keane, E. Kiritsis, A. Mischke, R. Mizuk, G. Odyniec, K. Papadodimas, A. Pich, R. Pittau, J.-W. Qiu, G. Ricciardi, C. A. Salgado, K. Schwenzer, N. G. Stefanis, G. M. von Hippel, and V. I. Zakharov, *Eur. Phys. J. C* **74**, 2981 (2014), [1404.3723 \[hep-ph\]](#).
 [16] M. Buballa, V. Dexheimer, A. Drago, E. Fraga, P. Haensel, I. Mishustin, G. Pagliara, J. Schaffner-Bielich, S. Schramm, A. Sedrakian, and F. Weber, *J. Phys. G* **41**, 123001 (2014), [arXiv:1402.6911 \[astro-ph.HE\]](#).
 [17] M. G. Alford, A. Schmitt, K. Rajagopal, and T. Schäfer, *Rev. Mod. Phys.* **80**, 1455 (2008), [arXiv:0709.4635 \[hep-ph\]](#).
 [18] R. Anglani, R. Casalbuoni, M. Ciminale, N. Ippolito, R. Gatto, M. Mannarelli, and M. Ruggieri, *Rev. Mod. Phys.* **86**, 509 (2014), [arXiv:1302.4264 \[hep-ph\]](#).
 [19] S. B. Rüster, V. Werth, M. Buballa, I. A. Shovkovy, and D. H. Rischke, *Phys. Rev.* **D72**, 034004 (2005), [arXiv:hep-ph/0503184 \[hep-ph\]](#).
 [20] D. Blaschke, S. Fredriksson, H. Grigorian, A. M. Öztaş, and F. Sandin, *Phys. Rev. D* **72**, 065020 (2005), [hep-ph/0503194](#).
 [21] D. Blaschke, F. Sandin, T. Klähn, and J. Berdermann, *Phys. Rev. C* **80**, 065807 (2009), [arXiv:0807.0414 \[nucl-th\]](#).
 [22] L. Bonanno and A. Sedrakian, *A&A* **539**, A16 (2012), [arXiv:1108.0559 \[astro-ph.SR\]](#).
 [23] H. J. Warringa, (2006), [arXiv:hep-ph/0606063 \[hep-ph\]](#).
 [24] K. Fukushima and T. Hatsuda, *Rep. Prog. Phys.* **74**, 014001 (2011), [arXiv:1005.4814 \[hep-ph\]](#).

- [25] M. Buballa, F. Neumann, M. Oertel, and I. Shovkovy, *Phys. Lett. B* **595**, 36 (2004), [nucl-th/0312078](#).
- [26] T. Klöhn, D. Blaschke, F. Sandin, C. Fuchs, A. Faessler, H. Grigorian, G. Röpke, and J. Trümper, *Phys. Lett. B* **654**, 170 (2007), [nucl-th/0609067](#).
- [27] T. Klöhn, R. Lastowiecki, and D. Blaschke, *Phys. Rev. D* **88**, 085001 (2013), [arXiv:1307.6996 \[nucl-th\]](#).
- [28] V. Dexheimer, R. Negreiros, and S. Schramm, *Phys. Rev. C* **91**, 055808 (2015), [arXiv:1411.4623 \[astro-ph.HE\]](#).
- [29] D. Alvarez-Castillo, S. Benić, D. Blaschke, S. Han, and S. Typel, *Eur. Phys. J. A* **52**, 232 (2016), [arXiv:1608.02425 \[nucl-th\]](#).
- [30] D. E. Alvarez-Castillo and D. Blaschke, *Phys. Part. Nucl.* **46**, 846 (2015), [arXiv:1412.8463 \[astro-ph.HE\]](#).
- [31] D. Alvarez-Castillo, A. Ayriyan, S. Benić, D. Blaschke, H. Grigorian, and S. Typel, *Eur. Phys. J. A* **52**, 69 (2016), [arXiv:1603.03457 \[nucl-th\]](#).
- [32] A. Zacchi, L. Tolos, and J. Schaffner-Bielich, *Phys. Rev. D* **95**, 103008 (2017), [arXiv:1612.06167 \[astro-ph.HE\]](#).
- [33] B. K. Agrawal and S. K. Dhiman, *Phys. Rev. D* **79**, 103006 (2009), [arXiv:0904.2946 \[astro-ph.HE\]](#).
- [34] S. Benić, D. Blaschke, D. E. Alvarez-Castillo, T. Fischer, and S. Typel, *A&A* **577**, A40 (2015), [arXiv:1411.2856 \[astro-ph.HE\]](#).
- [35] D. Blaschke, D. E. Alvarez-Castillo, and S. Benić, *Proc.Sci. CPOD* **063** (2013).
- [36] M. G. Alford, K. Rajagopal, S. Reddy, and F. Wilczek, *Phys.Rev.* **D64**, 074017 (2001), [arXiv:hep-ph/0105009 \[hep-ph\]](#).
- [37] L. F. Palhares and E. S. Fraga, *Phys.Rev.* **D82**, 125018 (2010), [arXiv:1006.2357 \[hep-ph\]](#).
- [38] M. B. Pinto, V. Koch, and J. Randrup, *Phys. Rev.* **C86**, 025203 (2012), [arXiv:1207.5186 \[hep-ph\]](#).
- [39] M. G. Alford, S. Han, and M. Prakash, *Phys. Rev. D* **88**, 083013 (2013), [arXiv:1302.4732 \[astro-ph.SR\]](#).
- [40] Z. F. Seidov, *Soviet Ast.* **15**, 347 (1971).
- [41] J. L. Zdunik and P. Haensel, *A&A* **551**, A61 (2013), [arXiv:1211.1231 \[astro-ph.SR\]](#).
- [42] G. Colucci and A. Sedrakian, *Phys. Rev. C* **87**, 055806 (2013), [arXiv:1302.6925 \[nucl-th\]](#).
- [43] M. Fortin, C. Providencia, A. R. Raduta, F. Gulminelli, J. L. Zdunik, P. Haensel and M. Bejger, *Phys. Rev. C* **94**, 035804 (2016) [[arXiv:1604.01944 \[astro-ph.SR\]](#)].
- [44] R. C. Tolman, *Phys. Rev.* **55**, 364 (1939).
- [45] J. R. Oppenheimer and G. M. Volkoff, *Phys. Rev.* **55**, 374 (1939).
- [46] J. M. Bardeen, K. S. Thorne, and D. W. Meltzer, *ApJ* **145**, 505 (1966).
- [47] N. K. Glendenning, S. Pei, and F. Weber, *Phys. Rev. Lett.* **79**, 1603 (1997), [astro-ph/9705235](#).
- [48] J. L. Zdunik, M. Bejger, P. Haensel, and E. Gourgoulhon, *A&A* **450**, 747 (2006), [astro-ph/0509806](#).
- [49] M. Bejger, D. Blaschke, P. Haensel, J. L. Zdunik, and M. Fortin, *A&A* **600**, A39 (2017), [arXiv:1608.07049 \[astro-ph.HE\]](#).
- [50] J. L. Zdunik, M. Bejger, P. Haensel, and E. Gourgoulhon, *A&A* **479**, 515 (2008), [arXiv:0707.3691](#).
- [51] H. Dimmelmeier, M. Bejger, P. Haensel, and J. L. Zdunik, *MNRAS* **396**, 2269 (2009), [arXiv:0901.3819 \[astro-ph.SR\]](#).
- [52] E. B. Abdikamalov, H. Dimmelmeier, L. Rezzolla, and J. C. Miller, *MNRAS* **392**, 52 (2009), [arXiv:0806.1700](#).
- [53] T. Fischer, I. Sagert, G. Pagliara, M. Hempel, J. Schaffner-Bielich, T. Rauscher, F.-K. Thielemann, R. Käppeli, G. Martínez-Pinedo, and M. Liebendörfer, *ApJS* **194**, 39 (2011), [arXiv:1011.3409 \[astro-ph.HE\]](#).
- [54] O. Heinimann, M. Hempel, and F.-K. Thielemann, *Phys. Rev. D* **94**, 103008 (2016), [arXiv:1608.08862 \[astro-ph.SR\]](#).
- [55] H. Sotani, K. Tominaga, and K. i. Maeda, *Phys. Rev. D* **65**, 024010 (2001) [[gr-qc/0108060](#)].
- [56] G. F. Marranghello, C. A. Z. Vasconcellos, and J. A. de Freitas Pacheco, *Phys. Rev. D* **66**, 064027 (2002) [[astro-ph/0208456](#)].
- [57] G. Miniutti, J. A. Pons, E. Berti, L. Gualtieri, and V. Ferrari, *Mon. Not. R. Astron. Soc.* **338**, 389 (2003) [[astro-ph/0206142](#)].
- [58] R. Oechslin, K. Uryu, G. S. Poghosyan, and F. K. Thielemann, *Mon. Not. R. Astron. Soc.* **349**, 1469 (2004) [[astro-ph/0401083](#)].
- [59] K. Takami, L. Rezzolla, and L. Baiotti, *Phys. Rev. Lett.* **113**, no. 9, 091104 (2014) [[arXiv:1403.5672 \[gr-qc\]](#)].
- [60] A. Bauswein and H.-T. Janka, *Phys. Rev. Lett.* **108**, 011101 (2012) [[arXiv:1106.1616 \[astro-ph.SR\]](#)].